Research Communication

Engineering Brown Fat into Skeletal Muscle Using Ultrasound-Targeted Microbubble Destruction Gene Delivery in Obese Zucker Rats: Proof of Concept Design

Raul A. Bastarrachea[1,2*]
Jiaxi Chen[3]
Jack W. Kent Jr.[1,2]
Edna J. Nava-Gonzalez[4]
Ernesto Rodriguez-Ayala[5]
Marcel M. Daadi[2]
Barbara Jorge[1,2]
Hugo Laviada-Molina[6]
Anthony G. Comuzzie[1,2]
Shuyuan Chen[7]
Paul A. Grayburn[7,8]

[1]*Department of Genetics, Texas Biomedical Research Institute, San Antonio, TX, USA*
[2]*Southwest National Primate Research Center, San Antonio, TX, USA*
[3]*University of Texas Southwestern Medical School, Dallas, TX, USA*
[4]*University of Nuevo Leon School of Nutrition and Public Health, Monterrey, Mexico*
[5]*Facultad de Ciencias de la Salud Universidad Anáhuac Norte, México DF, Mexico*
[6]*Escuela de Ciencias de la Salud Universidad Marista de Mérida, Yucatán, Yucatán*
[7]*Baylor Research Institute, Dallas, TX, USA*
[8]*Baylor University Medical Center, Dallas, TX, USA*

Abstract

Ultrasound-targeted microbubble destruction (UTMD) is a novel means of tissue-specific gene delivery. This approach systemically infuses transgenes precoupled to gas-filled lipid microbubbles that are burst within the microvasculature of target tissues via an ultrasound signal resulting in release of DNA and transfection of neighboring cells within the tissue. Previous work has shown that adenovirus containing cDNA of *UCP-1*, injected into the epididymal fat pads in mice, induced localized fat depletion, improving glucose tolerance, and decreasing food intake in obese diabetic mice. Our group recently demonstrated that gene therapy by UTMD achieved beta cell regeneration in streptozotocin (STZ)-treated mice and baboons. We hypothesized that gene therapy with *BMP7/PRDM16/PPARGC1A* in skeletal muscle (SKM) of obese Zucker diabetic fatty (*fa/fa*) rats using UTMD technology would produce a brown adipose tissue (BAT) phenotype with *UCP-1* overexpression. This study was designed as a proof of concept (POC) project. Obese Zucker rats were administered

Abbreviations: *ZDF, Zucker diabetic fatty; fa/fa, fatty mutation; UTMD, Ultrasound-targeted microbubble destruction; cDNA, complementary deoxyribonucleic acid; UCP-1, uncoupling protein-1; BMP7, bone morphogenetic protein 7; PRDM16, PR domain-containing protein16; PGC-1a/PPARGC1A, peroxisome proliferator-activated receptor gamma coactivator 1-alpha; SKM, skeletal muscle; BAT, brown adipose tissue; WAT, white adipose tissue; IHC, immunohistochemistry; OP, oxidative phosphorylation; RT-PCR, reverse transcription polymerase chain reaction; NPY, neuropeptide Y; POMC, pro-opiomelanocortin; SOCS3, suppressor of cytokine signaling 3; AMPK, AMP-activated protein kinase; mTOR, mammalian target of rapamycin; TRPV1, transient receptor potential vanilloid 1; NEFA, nonesterified fatty acids; PBS, phosphate-buffered saline; AU, arbitrary units*

P.A.G. and A.G.C. are senior co-authors.

Volume 69, Number 9, September 2017, Pages 745–755

**Address correspondence to: Raul A. Bastarrachea, Department of Genetics, Texas Biomedical Research Institute, 7620 NW Loop 410, San Antonio, TX 78227, USA. Tel: 210-258-9731.*
E-mail: raul@txbiomed.org

Received 27 May 2017; Accepted 9 July 2017
DOI 10.1002/iub.1658
Published online 31 July 2017 in Wiley Online Library (wileyonlinelibrary.com)

plasmid cDNA contructs encoding a gene cocktail with *BMP7/PRDM16/PPARGC1A* incorporated within microbubbles and intravenously delivered into their left thigh. Controls received UTMD with plasmids driving a *DsRed* reporter gene. An ultrasound transducer was directed to the thigh to disrupt the microbubbles within the microcirculation. Blood samples were drawn at baseline, and after treatment to measure glucose, insulin, and free fatty acids levels. SKM was harvested for immunohistochemistry (IHC). Our IHC results showed a reliable pattern of effective UTMD-based gene delivery in enhancing SKM overexpression of the *UCP-1* gene. This clearly indicates that our plasmid DNA construct encoding the gene combination of *PRDM16, PPARGC1A,* and *BMP7* reprogrammed adult SKM tissue into brown adipose cells *in vivo*. Our pilot established POC showing that the administration of the gene cocktail to SKM in this rat model of genetic obesity using UTMD gene therapy, engineered a BAT phenotype with *UCP-1* over-expression. © 2017 IUBMB Life, 69(9):745–755, 2017

Keywords: *gene therapy; UTMD; microbubbles; brown adipose tissue; UCP-1*

Introduction

The genetic basis of obesity is a process regulated by changes in expression of specific proteins; therefore, genetic defects within the corresponding coding or regulatory DNA sequences constitute its cellular and genomic foundations (1). New strategies for weight loss treatment and prevention of obesity-related comorbidities are urgently needed to successfully reverse or prevent the health complications caused by fat accumulation (2,3). Uncoupling protein-1 (UCP-1) is exclusively found in brown adipose tissue (BAT). Similar to skeletal muscle (SKM), BAT contains a much higher number of mitochondria compared with white adipose tissue (WAT) (4) and a specialized, specific UCP-1. This specialized protein uncouples ATP production from mitochondrial respiration and converts energy into heat. The manipulation of BAT is a promising and significant strategy in combating obesity, since it contributes to the regulation of whole-body energy expenditure (EE) and body fat content (5). Gene therapy is designed to transfer genetic material with the intent of providing therapeutic potential. Gene therapy commonly uses viral vectors as a viable solution for gene therapy delivery systems (6). However, biosafety concerns greatly limited viral vector application. In contrast, non-viral gene therapy offers gene delivery without potential complications of toxicity, altered immune response, and decreased capability to target specific cells (7,8). The focus of obesity-related gene therapy is to favor EE and lipolysis by modulating expression of appropriate gene targets to restore and maintain energy homeostasis. Exciting work in rodents has shown that adenovirus containing the cDNA of *UCP-1* induced localized fat depletion, improved glucose tolerance, and decreased food intake when injected into the epididymal fat pads of obese and diabetic mice. This increased fat combustion resulted from an increased expression of *UCP-1* in WAT. Generating new BAT via gene therapy is a promising approach (9,10).

Ultrasound-targeted microbubble destruction (UTMD) technology is a non-viral, novel approach to gene therapy in which plasmid DNA is targeted to specific tissues and organs *in vivo* (11). The UTMD technique has successfully driven expression of plasmid cDNA in rat (12) and baboon pancreatic islets, encoding pancreatic genes known to be involved in islet development (13). Our research group is the first to apply UTMD to the study of metabolic disorders in nonhuman primates (13). The delivery of genes by intravenously injecting plasmid DNA encapsulated in microbubbles into the animal's blood stream, to lyse them selectively in the microcirculation of specific organs via ultrasound, is highly innovative (14).

This proof of concept (POC) project was designed to determine whether the administration of a gene cocktail with *BMP7/PRDM16/PPARGC1A* in SKM of Zucker diabetic fatty (ZDF) (*fa/fa*) rats using UTMD technology will produce a BAT phenotype with *UCP-1* overexpression. This research proposal was based on recent findings which indicate that WAT and BAT have distinct developmental origins (15). A common lineage for SKM and BAT has been proposed different to WAT. Unlike white adipose cells that originate from Myf5 negative (–) precursors and are derived from blood vessel-associated pericyte-like cells, SKM and BAT are derived from precursors expressing the key myogenic factor Myf5 positive (+) (16). Adipogenesis is controlled by bone morphogenetic proteins (BMPs). BMP2 and 4 promote the development of WAT, whereas BMP7 promotes the development of BAT (17). BMP7 also induces the expression of *PRDM16* which functions to promote BAT gene expression and suppress the white fat program (18). The cascade of events is triggered as follows: precursor cells, positive for the muscle developmental gene Myf5, are stimulated by *BMP7* to express *PRDM16* which acts as a switch to instigate the brown fat differentiation pathway and inhibit the WAT and myogenic pathway. PRDM16 acts to induce the expression of *PPARGC1A*. Activation of *PPARGC1A* by BMP7 and PRDM16 drives a complete brown fat differentiation program and *UCP-1* expression, the hallmark of BAT (19).

In this POC pilot study, we showed that by administering tissue-specific UTMD gene therapy, we were able to obtain

overexpression of *UCP-1* in the SKM of ZDF *fa/fa* rats. Two rats received UTMD with plasmids driving *BMP7/PRDM16/PPARGC1A* genes, and two controls received UTMD with plasmids driving the *DsRed* reporter gene. We examined the cellular consequences of UTMD delivery of *BMP7/PRDM16/PPARGC1A* genes into SKM and showed that the gene cocktail converted this tissue into a brown fat phenotype, causing molecular changes to transform it into brown adipose-like, mitochondrial *UCP1*-abundant cells able to increase fat and glucose oxidation.

Materials and Methods

Experimental Animals

Obese ZDF (*fa/fa*) male rats were purchased from Charles River Laboratories, housed in a temperature-controlled environment under a 12:12-h light–dark cycle and were fed *ad libitum*. Animal facilities met the guidelines of the National Institutes of Health recommendations and the approval of our institutional animal research committee. Animals received regular chow for the length of the study. A total of four rats received: (1) UTMD with *pCMV-DsRed* plasmid ($n = 2$); (2) UTMD with a gene cocktail with *PRDM16, PPARGC1A*, and *BMP7* ($n = 2$). All genes were delivered as plasmid cDNA. *PRDM16* (pcDNA3.1, Catalog no. 15503, deposited by Bruce Spiegelman Lab.) and *PPARGC1A* (pcDNA4myc, Catalog no. 10974, deposited by Toren Finkel Lab.) were obtained from the nonprofit plasmid repository Addgene. *BMP7* (untagged-human *BMP7*) Catalog no. sc119058) was purchased from OriGene Technologies. Weight measurement was performed in the rats with an Ohaus-Valor 3000 XTREME scale. The thickness of subcutaneous (SQ) adipose tissue was determined by ultrasound image. Food intake was measured on a daily basis.

Manufacture of Plasmid-Containing Lipid-Stabilized Microbubbles

Lipid-stabilized microbubbles were prepared as described previously (13). Briefly, a stock solution is prepared containing 270 mg of 1,2-dipalmitoyl-Sn-glycero-3-phosphatidylcholine, (Sigma, St. Louis, MO), 30 mg of 1,2-dipalmitoyl-Sn-glycero-3-phosphatidylethanolamine, (Sigma, St. Louis, MO), and 1 g of glucose. These ingredients are dissolved in a boiling water bath for 20–30 min, with pipetting of contents up and down until no visible particles remain. This stock solution is stored at 4 °C. Plasmid containing microbubbles are prepared by mixing 2 mg of dried plasmid with 50 μL of lipofectamine 2000 (Invitrogen, Carlsbad, CA) and incubating at room temperature for 15 min. This liposome/plasmid DNA mixture is added to 250 mL of lipid stock solution, 50 mL of pure glycerol, and 5 μL of 10% albumin solution, mixed well with a pipette, and then placed in ice. Aliquots of 0.5 mL of this phospholipid–plasmid solution are placed in 1.5 mL clear vials; the air in the headspace of the vials is replaced with perfluoropropane gas (Air Products, Inc, Allentown, PA). Each vial is incubated at 4 °C for 30 min and then mechanically shaken for 30 sec by a dental amalgamator (VialmixTM, Bristol-Myers Squibb Medical Imaging, N. Billerica, MA). The lipid-stabilized microbubbles appear as a milky white suspension floating on the top of a layer of liquid containing unattached plasmid DNA. The subnatant is discarded and the microbubbles were washed three times with phosphate-buffered solution (PBS) to remove unattached plasmid DNA. The mean diameter and concentration of the microbubbles in the upper layer are measured by a particle counter (Beckman Coulter Multisizer III).

Delivery of Plasmid cDNA Contructs Encoding the Gene Cocktail with *BMP7/PRDM16/PPARGC1A* into the Left Thigh of the Rats

The microbubbles were infused intravenously under anesthesia. The microbubble suspension (driving the gene cocktail with *BMP7/PRDM16/PPARGC1A*) or control solutions (0.5 mL diluted with 0.5 mL PBS) were infused over 5 min via pump (Genie, Kent Scientific). Plasmid DNA containing the reporter gene *DsRed* or the functional gene cocktail construct under the regulation of a cytomegalovirus promoter was incorporated within the phospholipid shell of perfluoropropane gas-filled microbubbles. These plasmid constructs with routine plasmid vectors were isolated with cloning techniques and gene promoter construction. The plasmid-containing lipid-stabilized microbubbles were prepared following procedures described previously (13). During this infusion, a commercially available ultrasound transducer (S3 probe, Sonos 5500, Philips Ultrasound, Bothell, WA) was directed to the right thigh of the treated and control rats to disrupt the microbubbles within the microcirculation. The probe was clamped in place. Ultrasound was then applied in ultraharmonic mode (transmit 1.3 MHz/receive 3.6 MHz) at a mechanical index of 1.4. Four bursts of ultrasound were triggered to every fourth end-systole by electrocardiogram using a delay of 45–70 msec after the peak of the R wave. These settings have shown to be optimal for plasmid delivery by UTMD using this instrument (20). Microbubble destruction was visually apparent in all rats. Blood samples were drawn after an overnight 12 h fast at baseline and after treatment. Blood glucose levels were measured; blood insulin and free fatty acids (FFA) were measured with RIA kit (Linco Research, Radioimmunoassay). SKM was harvested for histology. Muscle tissue was collected from the left (treated) and right (control) thighs (vastus lateralis) in all animals. All samples were placed in weigh boats and delivered to the processing room by the surgical technicians immediately following collection.

Immunohistochemistry

We fixed and processed tissues for immunohistochemistry (IHC). The detection of UCP-1, PRDM16, BMP7, PGC-1alpha, and perilipin from muscle tissue was assayed as follows: cryostat sections 5 μm in thickness were fixed in 4% paraformaldehyde for 15 min at 4 °C and quenched for 5 min with 10 mM glycine in PBS. Sections were then rinsed in PBS three times and permeabilized with 0.5% Triton X-100 in PBS for 10 min. Sections were blocked with 10% vol_vol goat serum at 37 °C for 1 h and washed three times with PBS. The primary

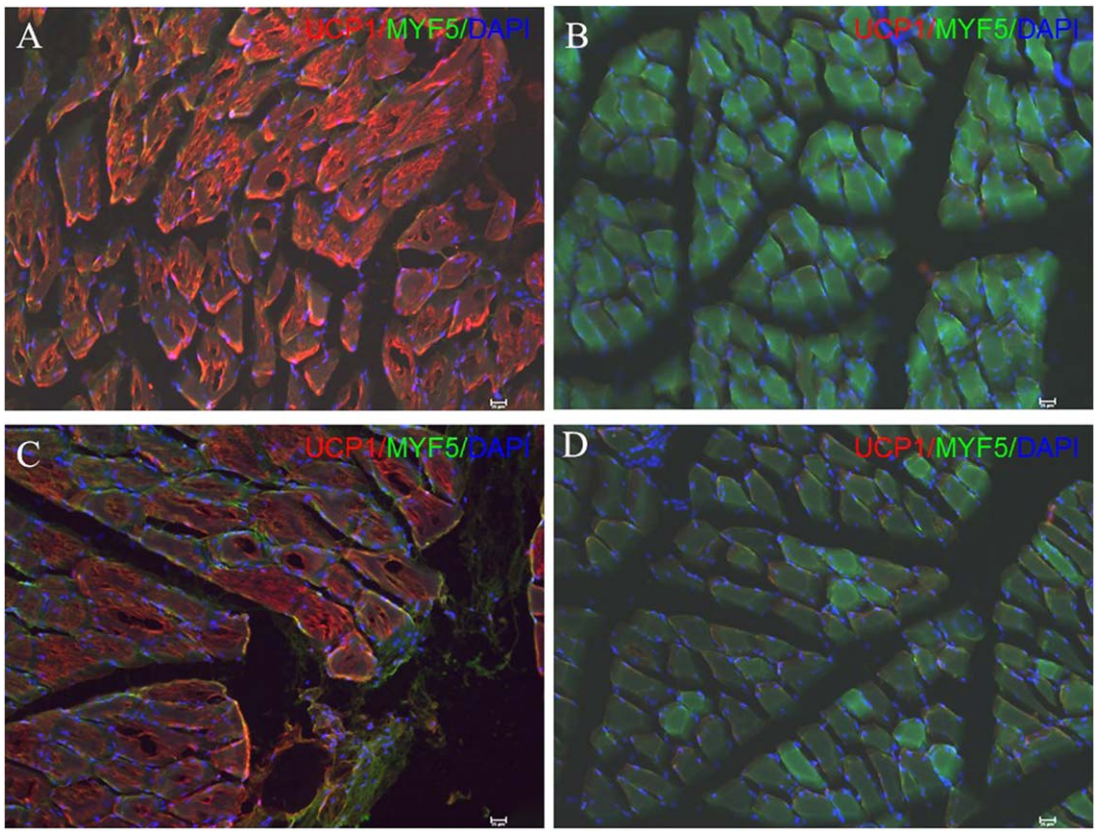

FIG 1 *Triple staining for muscle tissue in the left thigh at magnification of ×200. Robust in vivo UCP-1 signaling from BAT in SKM after UTMD.*

antibodies (rabbit polyclonal UCP-1 antibody, rabbit polyclonal PRDM16 antibody, rabbit polyclonal BMP7 antibody, rabbit polyclonal PGC-1alpha antibody, rabbit polyclonal perilipin antibody, and mouse recombinant monoclonal Myf5 antibody [OriGene Technologies]) were added and incubated at 4 °C overnight. After washing with PBS three times for 5 min each time, the secondary antibody was added and incubated for 1 h at 37 °C. Sections were rinsed five times with PBS for 10 min each time and then mounted. 4′,6-diamidino-2-phenylindole (1:5,000 dilution). The images were taken by Leica confocal microscope TCS SP5.

Real Time RT-PCR analysis

Rat brain slices were obtained after euthanasia at the end of the study to perform real time reverse transcription polymerase chain reaction (RT-PCR; TaqMan assays, ThermoFisher Technologies) and detect key hypothalamic genes influencing energy balance (*NPY, POMC,* and *SOCS3*) and nutrient-sensing (AMP-activated protein kinase [*AMPK*], *mTOR,* and *TRPV1)* using an ABI PRISM 7900 HT sequence detection system (Life Technologies Corporation, Carlsbad, CA).

Subcutaneous Abdominal Fat Thickness Measurement with Ultrasound Image

An anatomical area in all four Zucker rats was carefully defined on the left lateral wall of the abdomen. This area was clipped and a reading was obtained with an A-mode device using a focused transducer with a resonant frequency of 20 MHz (Sonos 5500, Philips Ultrasound, Bothell, WA). The thickness of the subcutaneous abdominal fat layer was then calculated immediately after ultrasonic investigation.

Data Analysis

The primary endpoint of the POC study was to find out whether gene therapy with *BMP7/PRDM16/PPARGC1A* in SKM of obese ZDF (*fa/fa*) rats using UTMD technology would produce a BAT phenotype with *UCP-1* overexpression. Then, we decided to describe the trend from observations regarding short-term changes in food consumption, fat mass evaluation with ultrasound image (subcutaneous abdominal fat thickness [SFT]), as well as key metabolic parameters (insulin, glucose, and fatty acids) between the treated *versus* control obese Zucker rats as a secondary objective. Even though the sample size is small for formal statistical tests, the dispersion of mean change in these parameters (Fig. 4) strongly suggests metabolic alterations consistent with *UCP-1* overexpression. Gene expression for hypothalamic genes involved in energy homeostasis and nutrient-sensing was calculated using the nonparametric Mann-Whitney U (rank-sum) test. Graphics and statistical analysis were carried out using GraphPad Prism V 6.07.

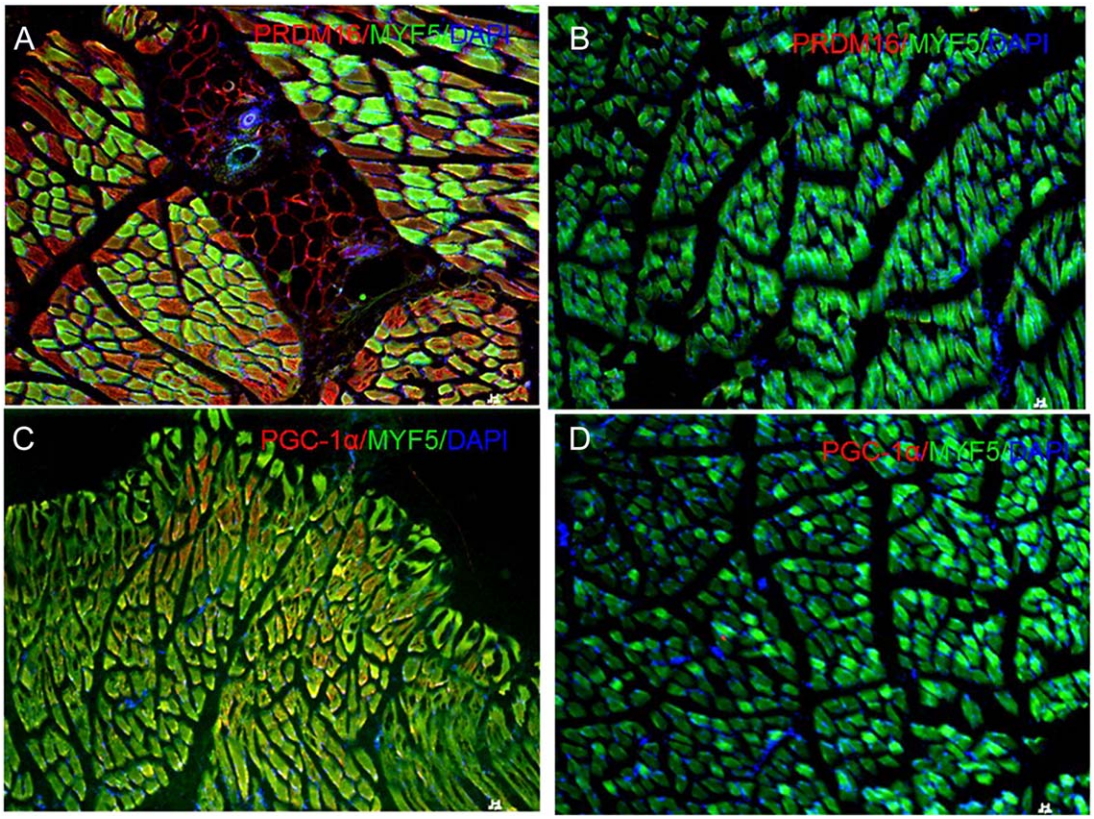

FIG 2 *Myf5+ in SKM cells transdifferentiating into BAT with strong PRDM16 (A) and a fairly noticeable PGC-1alpha signaling (C). PRDM16 acts to induce the expression of PGC-1alpha.*

Results

To establish POC that UTMD is an effective method for *in vivo* plasmid-based gene transfer in SKM, we administered a construct into the SKM of four male ZDF *(fa/fa)* rats (56 days old), a spontaneous genetic obesity model which exhibits hyperphagia, hyperglycemia, hyperinsulinemia, and hyperlipidemia. Intravenous microbubbles carrying plasmids with a cocktail of *BMP7/PRDM16/PPARGC1A* genes were burst within the microcirculation of the left thigh by ultrasound (treated muscle) in two rats, achieving local gene expression after targeting our specific tissue. We were able to clearly demonstrate the ability to disrupt microbubbles and release the plasmids with the gene cocktail. We used the muscle of the right thigh as a control site in another two rats, administering UTMD with plasmids driving the *DsRed* reporter (marker) gene. We collected muscle tissue from the left (treated) and right (control) thighs in all four ZDF (*fa/fa*) rats. Our POC pilot lasted 30 days with a 20-day period of UTMD gene therapy.

We performed confocal microscopy with FITC-labeled anti-UCP-1, DsRed-labeled anti-Myf5, and anti-perilipin for IHC. Figure 1A,C shows triple staining for muscle tissue in the left thigh at magnification of ×200. Anti-UCP-1 (red) and anti-Myf5 (green) antibodies were used. Strong detection by IHC of *UCP-1* expression indicates that the gene combination of *PRDM16, PPARGC1A*, and *BMP7* reprogrammed adult SKM into brown adipose cells after UTMD *in vivo* by day 10 (Fig. 1A) and 20 (Fig. 1C), respectively. Figure 1B,D show a strong detection of Myf5+ (green) and no UCP-1 signal detected in the right thigh of the control rats (magnification at ×100). Figure 2A clearly shows precursors Myf5+ in SKM cells transdifferentiated into mature brown adipose cells in the muscle of the left thigh in the treated rats. Clear signals for PRDM16 (red) (Fig. 2A) and PGC-1alpha (red) (Fig. 2C) are identified. Figure 2B,D shows no detection of *PRDM16* and *PPARGC1A* activity in the muscle of the right thigh of control animals. Figure 3A,B shows presence in the muscle of the left thigh in treated rats and absence in the muscle of the right thigh in control rats of *BMP7* activity. Figure 3C shows the presence of perilipin antibody, a marker of adipose cells, detected at day 20 post UTMD gene delivery in the left thigh of treated rats. There is an absence of activity for perilipin in the muscle of the right thigh in control animals in Fig. 3D.

All rats were receiving 132 kcal/day of regular chow pellets (Harlan rodent diet #2919, 3.3 kcal/g). Figure 4A shows that their regular intake before UTMD gene therapy was ~109 kcal/day. Daily food intake acutely decreased to ~39.6 kcal/day within the first 4 days after UTMD gene therapy in our treated rats. These rats under *PRDM16, PPARGC1A*, and *BMP7* gene therapy administration gradually increased their daily food intake, recovering the intake levels previous to UTMD

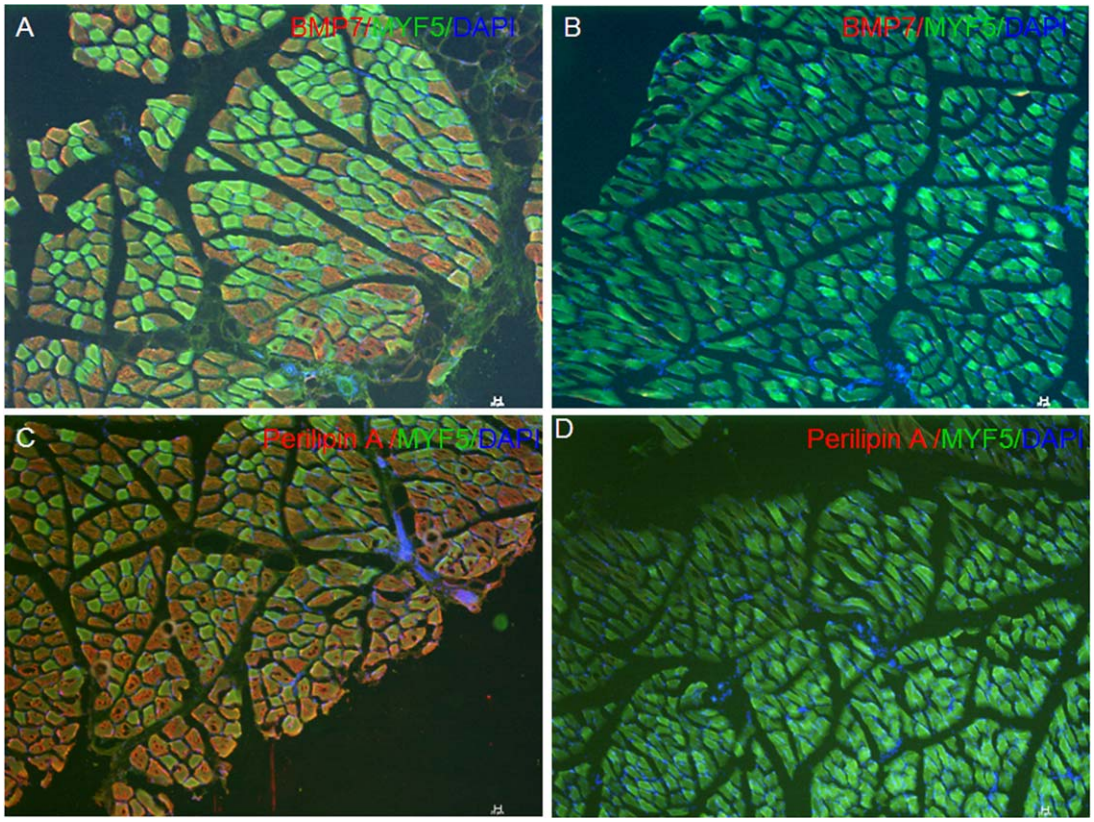

FIG 3 *Presence of BMP7 in SKM and perilipin activity at day 20 post UTMD gene therapy. BMP7 induces the expression of PRDM16 which functions to promote BAT gene expression and suppress the white fat program.*

gene therapy by day 20. Figure 4B shows that all rats were gaining equal weight previous to UTMD gene therapy as expected (up to ~50 g). However, the treated rats experienced a sudden weight loss of ~25 g in the first 4 days after UTMD gene therapy. Their controls gained ~30 g within the same period of time. By day 20, treated rats reached a final weight of ~90 g despite having recovered the same amount of food intake previous to UTMD gene therapy administration *versus* their controls reaching ~225 g (135 g difference).

Figure 4C shows that the weight loss from the treated rats as a mean of fat thickness evaluated with ultrasound image resulted in a greater percentage from fat mass (loss of −0.1 cm by day 10 and a regain to 0.05 cm by day 20), compared with controls (steady gain of 0.3 cm in 20 days). Figure 4D shows that the change (Δ) in glucose circulating levels in the non-treated control animals steadily rose up to 100 mg/dL by day 20. The (Δ) blood glucose levels in the treated animals kept a low and steady level of ~12.5 mg/dL during the same period of days. Figure 4E shows that the (Δ) insulin levels were lower by day 20 (–1,250 mIU/L) in the treated rats compared with the (Δ) insulin levels (–650 mIU/L) found in the controls. Figure 4F shows the same pattern for the (Δ) NEFA circulating levels: −0.15 mEq/L in the controls *versus* −0.25 mEq/L in the treated rats at day 20.

Figure 6 shows the pattern of expression we obtained from rat brain tissue at day 20. The differential expression of key genes involved in appetite control and nutrient sensing (*NPY*, *POMC, TRPV1,* and *AMPK*) were not significant. However, for two key genes, the levels of expression was higher in the treated animals (*SOCS3* levels of expression in treated 1.4 AU *vs*. controls 1.15 AU, and *mTOR* 1.3 AU levels in the treated *vs*. 1.2 AU levels in the controls).

Discussion

This study was primarily designed to establish POC showing that the administration of a gene combination of *BMP7/PRDM16/PPARGC1A* to SKM in this rat model of genetic obesity using UTMD gene therapy engineered a BAT phenotype with *UCP-1* over-expression.

Gene therapy-based approaches for obesity focus on the transfer of gene coding or non-coding sequences to produce critical proteins to re-establish metabolic homeostasis. The potential application for gene therapy in treating obesity has led to efforts centered on regulated expression using different methods such as viral, non-viral, and synthetic delivery systems (21). UTMD, as a means of non-viral tissue-specific gene delivery, attaches plasmid DNA vectors encoding a gene of interest to shells of gas-filled lipid microbubble contrast agents. Several key metabolic tissues have been targeted with this UTMD gene delivery technique such as pancreas, adipose tissue, kidney, heart, endothelium, and SKM (22,23).

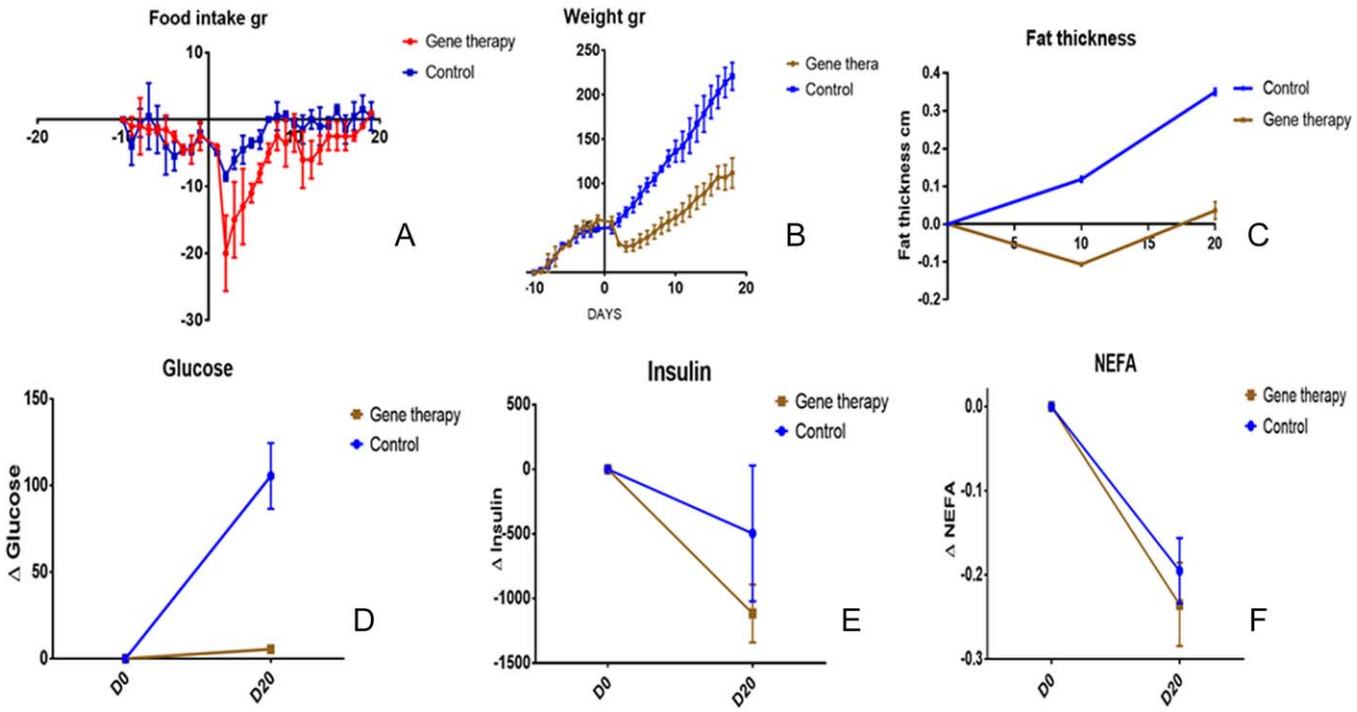

FIG 4

(A) Changes from baseline in food intake (g), (B) body weight (g), and (C) fat thickness (cm) Zucker rats. Error bars represent standard deviation (SD). The functional metabolic result of overexpressing UCP-1 in SKM observed in this figure nicely correlated with hypophagia, and circulating levels of (D) glucose (mg/dL), (E) insulin, and (F) fatty acids (NEFA) in treated versus *control weight loss and metabolic improvement in the treated obese ZDF* (fa/fa) *rats for a short period of days.*

Our IHC results showed a reliable pattern of effective UTMD-based gene delivery in enhancing SKM overexpression of the *UCP-1* gene (Fig. 1A and C). The data obtained seem to suggest that our systemic gene delivery via UTMD, by increasing local concentration of our transgene *BMP7/PRDM16/PPARGC1A* cocktail (Figs. 1 and 2), allowed for efficient transfection (via cavitation and tissue pore formation, through ultrasound application and microbubble destruction), and was capable of switching the precursor cell lineage and regulatory myogenic factors for SKM development into the molecular machinery necessary to establish a terminally differentiated BAT and *UCP-1* overexpression *in vivo*. Our group has obtained similar results recently demonstrating that a single UTMD treatment delivered to pancreatic islets of STZ-treated rats with a cell cycle regulation gene cocktail cyclin D2/CDK4/glucagon-like peptide 1 (*CCND2/CDK4/GLP-1*), resulted in durable induction of β-cell regeneration without evidence of toxicity (12). We have also generated important preliminary data indicating that gene therapy by UTMD using the same cell cycle regulation gene cocktail can achieve *in vivo* evidence of islet regeneration and restoration of β-cell mass in baboons (13).

Our POC results may support that from an evolutionary perspective, the ability of BAT to produce facultative thermogenesis became so important that its contractile components disappeared, although the very small, rapidly mobilizable lipid droplets remained, ATP synthesis disappeared, large amounts of mitochondria with a strong expression of the nuclear gene *UCP-1*, the uncoupler of oxidative phosphorylation responsible for non-shivering thermogenesis appeared, and a thermogenic tissue of myogenic origin developed (24). Hence, some authors currently consider BAT as a kind of specialized muscle (4).

We also observed interesting short-term changes in food consumption, fat mass evaluation with ultrasound image (SFT), as well as key metabolic parameters (insulin, glucose, and fatty acids) between the treated *versus* control obese Zucker rats. As shown in the results, the treated rats acutely decreased their daily food intake during the 4 days following gene therapy administration with the cell cycle regulation gene cocktail, compared with the controls. They gradually recover their food intake patterns to the levels shown previous to UTMD gene therapy. All experimental animals experienced the expected weight gain seen in a Zucker rat before UTMD gene therapy. However, the weight pattern in the treated rats showed a sudden weight loss within the same four days after UTMD gene therapy, unlike their controls which kept gaining weight during the same period of time. Interestingly, the treated rats reached much less weight regain compared with their controls by day 20 in spite of having recovered the same amount of food intake previous to UTMD gene therapy administration (Fig. 4A,B). The loss of SFT with ultrasound image in the treated Zucker rats was evident when compared with the steady subcutaneous abdominal fat gain shown in the control animals (Fig. 4C). The glucose, insulin, and NEFA showed low

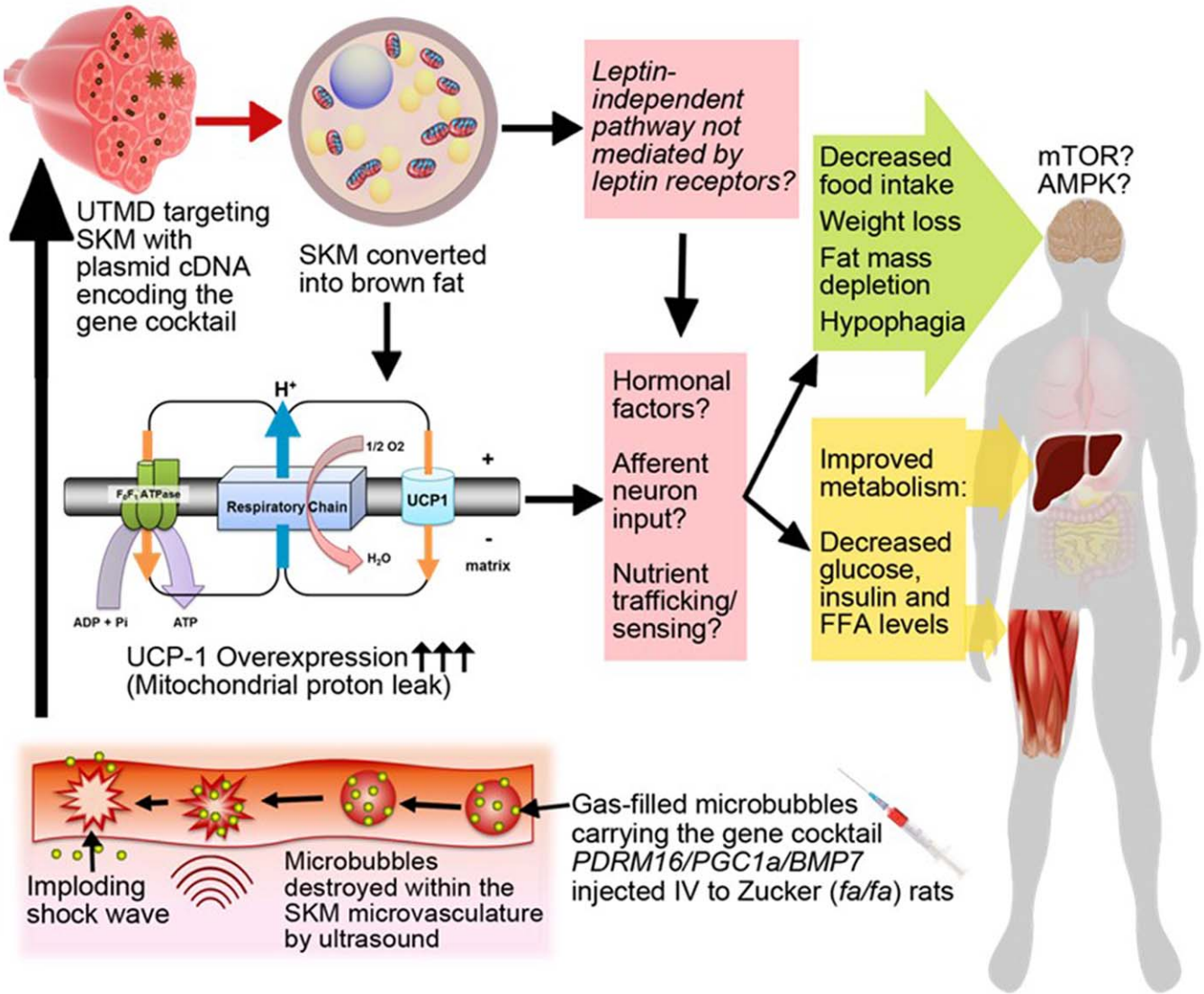

FIG 5 *A hypothetical mechanism by which gene therapy with BMP7/PRDM16/PPARGC1A in SKM of obese ZDF (*fa/fa*) rats using UTMD technology would produce a BAT phenotype with UCP-1 overexpression leading to nutrient trafficking/sensing and an energy gap, mediating hypophagia and metabolic improvement not regulated by leptin receptors.*

circulating levels in the UTMD gene therapy treated rats after the administration of the UTMD gene cocktail by day 20 when compared with the expected elevated circulating levels of these three biomarkers measured in the control animals in the same day (Fig. 4D–F).

These observations show that the functional metabolic result of overexpressing *UCP-1* in SKM nicely correlated with hypophagia, weight loss, and metabolic improvement in the treated obese ZDF (*fa/fa*) rats for a short period of days (Fig. 4A–F). They suggest that by administering the vector-carrying microbubbles containing the cDNA of *BMP7/PRDM16/PPARGC1A* into SKM an uncoupling of fatty acid and glucose oxidation from ectopic *UCP-1* overexpression may have been enhanced. What we obtained was a localized level of expression of *UCP-1* only in SKM surrounding the site of the thigh exposed to ultrasound implementation in the treated rats (Figs. 1–3). The food intake of the treated rats markedly declined for a few days correlating with weight loss and fat mass decrease in the same rats when compared with their controls. Fat thickness evaluated by ultrasound, insulin, and free fatty acid circulating levels were lower in the treated rats overexpressing *UCP-1* at day 20. In particular, fasting blood glucose was remarkably lower in these animals. These observed effects could reflect a transient correction of metabolic abnormalities in this obese, diabetic rat model. Therefore, we could assume that a limited and confined amount of *UCP-1* overexpression in SKM improved systemic insulin sensitivity, serum lipid parameters, and decreased fat mass accumulation, resulting in metabolic improvement of the diabetic phenotype in congenital leptin receptor-deficient ZDF (*fa/fa*) fatty rats.

These results are similar to the ones previously reported in wild type (C57BL/6) obese diabetic mice models, where

adenovirus containing the cDNA of *UCP-1* was delivered into the epididymal adipose tissue to induce fat depletion, resulting in a marked decrease in food intake (10). Interestingly, in this particular study, the researchers reported that the hypophagia found in the wild-type obese mice overexpressing *UCP-1* from the epididymal fat pads could not be duplicated in the *db/db* mice model with nonfunctioning and mutant leptin receptors, concluding that such hypophagia was leptin-signaling dependent. They also found improvement in blood glucose, insulin, triglyceride and fatty-acid levels, glucose tolerance, and insulin sensitivity in both the wild type and the *db/db* congenital model, concluding that the metabolic improvements observed were independent of the leptin signaling pathway (10).

In our study, it is worth noting that the obese ZDF (*fa/fa*) fatty rats carrying an equivalent missense mutation in the leptin receptor gene as in the *db/db* mice, also overexpressed *UCP-1*, but from SKM. They became transiently hypophagic, lost weight and fat mass, and their blood glucose, insulin and FFA markedly improved. We speculate that perhaps the reason for the anorectic response and metabolic improvement observed in our ZDF (*fa/fa*) rats with nonfunctional and mutant leptin receptors, as it was observed in the wild-type mice but not in the *db/db* model (10), may be related to the fact that the site of *UCP-1* overexpression in our congenital obese rats was SKM, not WAT, also occurring without the presence of a functional leptin signaling pathway.

Of note, leptin-resistant states due to loss-of-function mutations of the leptin receptor cause severe lipotoxicity. The ZDF *fa/fa* rats are the most extensively studied model of congenital leptin resistance, caused by a loss-of-function in the leptin receptor (25). The lack of leptin action on their thermogenic centers in the hypothalamus leads rapidly to obesity. Appetite, adipose tissue mass and plasma FFA increase steadily in these animals, leading to triglyceride accumulation in SKM, liver, pancreas and kidneys (26). We were able to ameliorate to some extent and for a short period of time these metabolic derangements with *UCP-1* overexpression through UTMD-based gene therapy in SKM in our Zucker *fa/fa* congenital rat model. Therefore, an interesting challenge arising from these POC preliminary results is to determine the molecular mechanisms underlying the hypophagia and the positive metabolic effects triggered through a single *UCP-1* overexpression in these ZDF (*fa/fa*) rats.

It is important, however, to bear in mind that this is a limited POC pilot study which needs to be interpreted carefully. All data gathered from this protocol will be used to design larger confirmatory studies and dictate the future direction of our research. This will include replicating this protocol in wild type rats and/or non-human primates using a calorie-dense palatable diet to induce them to become obese. We will collect EE data, body temperature, and measure BAT thermogenesis using infrared imaging and RT-PCR techniques to detect *UCP-1* activity *in vivo* (27). Another limitation of this POC pilot study was the number of treated *vs*. control ZDF (*fa/fa*) rats ($N = 4$). One more limitation was the lack of measurements of daily

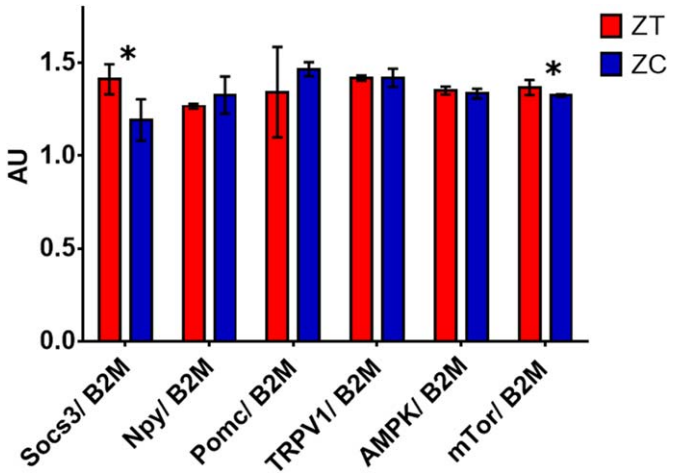

FIG 6

Pattern of expression obtained through RT-PCR of key hypothalamic genes involved in energy homeostasis (NPY, POMC, and SOCS3), and nutrient-sensing (AMPK, mTOR, and TRPV1) at day 20 post UTMD gene therapy. Red bars: treated Zucker rats. Blue bars: control Zucker rats.

EE. Indeed, if the reason to induce BAT thermogenesis through gene therapy is to achieve weight loss, hypophagia, and metabolic improvement, a fundamental question would be how much EE would have to occur with our UTMD gene therapy approach to reach clinically successful outcomes. This leads to another equally important question of how much mass of BAT should be induced in excess of what mammals normally possess to achieve appropriate metabolic improvement without producing deleterious side effects. Total volume of BAT in most humans has been reported in the range of 100–200 grams (28). The answers to these questions remain to be elucidated.

Nevertheless, our study documents the feasibility of UTMD gene-base therapy administration in SKM, the overexpression of *UCP-1* by IHC after delivery of the transgene *BMP7/PRDM16/PPARGC1A* cocktail, transient hypophagia, weight loss, SQ fat mass depletion measured through ultrasound, and improvement of insulin sensitivity and key metabolic parameters such as circulating FFA and glucose. Taken together, these findings may suggest that the metabolic improvement and weight loss may not have been mediated by leptin receptors from the hypothalamic leptin signaling pathway, since it occurred in the ZDF (*fa/fa*) rat. Therefore, we speculate that an anoretic action combined with a metabolic effect could have been triggered by a single administration of UTMD-based transgenes and localized *UCP-1* overexpression in SKM, achieved independently of the leptin signaling pathway (Fig. 5).

While the biological mechanisms underlying the short-term anorexigenic and metabolic effects obtained in this study remain to be unraveled, the results seem to indicate that the SKM, if genetically engineered, possesses the molecular capability to fully regulate calorie intake, substrate trafficking, and central and peripheral metabolism. Therefore, perhaps the

observed metabolic and anorexigenic effects could be mediated by cellular pathways related to nutrient-sensing homeostatic mechanisms (29). Indeed, recent findings seem to indicate that AMPK and mammalian target of rapamycin (mTOR), two interconnected major junctions playing key roles in metabolism, have a major impact in the control of brown adipogenesis process, nutrient-sensing and regulation of energy balance (29).

We tried to explore this possibility by analyzing key hypothalamic genes involved in energy homeostasis (*NPY, POMC,* and *SOCS3)* and nutrient-sensing (*AMPK, mTOR,* and *TRPV1)* through RT-PCR in our treated and control animals (30–32). Figure 6 shows the pattern of expression we obtained. Although we did not find significance differences, we did notice a slight increase in *SOCS3* and *mTOR* expression in the treated animals which appears to correlate with the recovery of food ingestion and the more pronounced weight loss, perhaps related to an overwhelming substrate trafficking secondary to the transient *UCP-1* over activity in SKM from days 10 to 20 after UTMD gene therapy. Indeed, recent scientific evidence suggests that circulating substrates (macronutrients such as fatty acids and amino acids) have specific actions to activate receptors and signaling pathways, in addition to providing fuel and essential nutrients. They can exert their effects on target tissues such as the hypothalamus by acting on cell-surface receptors through intracellular signaling cascades or via nuclear receptors to regulate gene transcription (33). Based on this evidence and our preliminary results, we could speculate that a measurement of these hypothalamic genes at an earlier time of the study would have given perhaps a more rational picture on behalf of our leptin-independent nutrient-sensing homeostatic working hypothesis explaining the hypophagia, weight loss and fat mass depletion.

A final intriguing observation was the curve of food intake and weight loss in the treated rats (Fig. 4A,B). These animals gradually recovered their food intake patterns by day 20, when compared with the patterns they showed before UTMD gene therapy administration and to the food intake of their controls. The weight loss in the treated rats never recovered the levels observed in the controls despite food intake recovery. This finding may be associated with the new "energy gap" concept (34). As an example, the Swedish Obesity Subjects (SOS) trial (35) showed that the efficacy of bariatric surgery to long-term weight loss is about 20 kg on average over 10–15 years. An analysis of the fall in EE for long-term weight loss achieved by bariatric surgery in the SOS trial seems to have been effective in stimulating daily EE by approximately 600 kcal daily (considered the energy gap for long-term maintenance, and subdivided into components that represent passive [obligatory] and active [adaptive thermogenesis] components), assuming no change in energy intake (36). Given that an increase in 24-h EE documented from any thermogenic compound at a safe dose is less than 150 kcal/day, a valid question would be whether the human body is able to reach a thermogenic capacity from BAT to achieve similar long-term weight loss as the one obtained in the SOS trial (37). In our POC study, the food intake and weight curves from days 0 to 20 after the administration of the gene cocktail of *BMP7/PRDM16/PPARGC1A* to treated Zucker rats (Fig. 4A,B) may reflect the energy gap hypothesis, where EE through BAT over activity secondary to UTMD gene therapy in muscle could have avoided weight regain in spite of the gradual recovery of their food intake patterns.

In conclusion, the preliminary results obtained in this POC pilot project may open a window to future innovative therapeutic strategies through gene therapy to treat and prevent cardiometabolic risk factors related to nutrition.

References

[1] Zolotukhin, S. (2005) Gene therapy for obesity. Expert Opin. Biol. Ther. 5, 347–357. PMID: 15833072

[2] Flegal, K. M., Graubard, B. I., Williamson, D. F., and Gail, M. H. (2007) Cause-specific excess deaths associated with underweight, overweight, and obesity. JAMA 298, 2028–2037. PMID: 17986696

[3] Hammond, R. A., and Levine, R. (2010) The economic impact of obesity in the United States. Diabetes Metab. Syndr. Obes. 3, 285–295. PMID: 21437097

[4] Farmer, S. R. (2008) Brown fat and skeletal muscle: unlikely cousins? Cell 134, 726–727. PMID: 18775306

[5] Ginter, E., and Simko, V. (2012) Brown fat tissue—a potential target to combat obesity. Bratisl Lek Listy 113, 52–56. PMID: 22380505

[6] Huang, Y., Liu, X., Dong, L., Liu, Z., He, X., et al (2011) Development of viral vectors for gene therapy for chronic pain. Pain Res. Treat. 2011, 968218. PMID: 22110937

[7] Niidome, T., and Huang, L. (2002) Gene therapy progress and prospects: non-viral vectors. Gene Ther. 9, 1647–1652. PMID: 12457277

[8] Wang, W., Li, W., Ma, N., and Steinhoff, G. (2013) Non-viral gene delivery methods. Curr. Pharm. Biotechnol. 14, 46–60. PMID: 23437936

[9] Unger, R. H., and Elmquist, J. K. (2006) Movin' on up: adipocytes become regulators of nutrient homeostasis. Cell Metab. 3, 147–148. PMID: 16517400

[10] Yamada, T., Katagiri, H., Ishigaki, Y., Ogihara, T., Imai, J., et al (2006) Signals from intra-abdominal fat modulate insulin and leptin sensitivity through different mechanisms: neuronal involvement in food-intake regulation. Cell Metab. 3, 223–229. PMID: 16517409

[11] Chen, S., Yang, F., Lin, Y., Zhang, J. S., Qiu, R. X., et al (2013) New development and application of ultrasound targeted microbubble destruction in gene therapy and drug delivery. Curr. Gene Ther. 13, 250–274. PMID: 23721204

[12] Chen, S., Shimoda, M., Chen, J., Matsumoto, S., Grayburn, P. A. (2012) Transient overexpression of cyclinD2/CDK4/GLP1 genes induces proliferation and differentiation of adult pancreatic progenitors and mediates islet regeneration. Cell Cycle 15:11, 695–705. PMID: 22373529

[13] Chen, S., Bastarrachea, R. A., Roberts, B. J., Voruganti, V. S., Frost, P. A., et al (2014) Successful beta cells islet regeneration in streptozotocin-induced diabetic baboons using ultrasound-targeted microbubble gene therapy with cyclinD2/CDK4/GLP1. Cell Cycle 13, 1145–1151. PMID: 24553120

[14] Vu, V., Liu, Y., Sen, S., Xu, A., and Sweeney, G .(2013) Delivery of adiponectin gene to skeletal muscle using ultrasound targeted microbubbles improves insulin sensitivity and whole body glucose homeostasis. Am. J. Physiol. Endocrinol. Metab. 304, E168–E175. PMID: 23132298

[15] Peirce, V., Carobbio, S., and Vidal-Puig, A. (2014) The different shades of fat. Nature 510, 76–83. PMID: 24899307

[16] Seale, P., Bjork, B., Yang, W., Kajimura, S., Kuang, S., et al (2008) PRDM16 controls a brown fat/skeletal muscle switch. Nature 454, 961–967. PMID: 18719582

[17] Tseng, Y. H., Kokkotou, E., Schulz, T. J., Huang, T. L., Winnay, J. N., et al (2008) New role of bone morphogenetic protein 7 in brown adipogenesis and energy expenditure. Nature 454, 1000–1004. PMID: 18719589

[18] Kajimura, S., Seale, P., Tomaru, T., Erdjument-Bromage, H., Cooper, M. P., et al (2008) Regulation of the brown and white fat gene programs through a

PRDM16/CtBP transcriptional complex. Genes Dev. 22, 1397–1409. PMID: 18483224
[19] Christian, M., and Parker, M. G. (2010) The engineering of brown fat. J. Mol. Cell Biol. 2, 23–25. PMID: 19825852
[20] Zhou, Q., Brown, J., Kanarek, A., Rajagopal, J., and Melton, D. A. (2008) *In vivo* reprogramming of adult pancreatic exocrine cells to beta-cells. Nature 455, 627–632. PMID: 18754011
[21] Nayerossadat, N., Maedeh, T., and Ali, P. A. (2012) Viral and nonviral delivery systems for gene delivery. Advanced Biomedical Research 1, 27. PMID: 23210086
[22] Mayer, C. R., Geis, N. A., Katus, H. A., and Bekeredjian, R. (2008) Ultrasound targeted microbubble destruction for drug and gene delivery. Expert Opin. Drug Deliv. 5, 1121–1138. PMID: 18817517
[23] Wang, X., Liang, H. D., Dong, B., Lu, Q. L., and Blomley, M. J. (2005) Gene transfer with microbubble ultrasound and plasmid DNA into skeletal muscle of mice: comparison between commercially available microbubble contrast agents. Radiology 237, 224–229. PMID: 16081853
[24] Mezentseva, N. V., Kumaratilake, J. S., and Newman, S. A. (2008) The brown adipocyte differentiation pathway in birds: an evolutionary road not taken. BMC Biol. 6, 17.
[25] Lida, M., Murakami, T., Ishida, K., Mizuno, A., Kuwajima, M., et al (1996) Substitution at codon 269 (glutamine-proline) of the leptin receptor (OB-R) cDNA is the only mutation found in the Zucker Fatty (fa/fa) rat. Biochem. Biophys. Res. Commun. 224, 597–604. PMID: 8702432
[26] Pelleymounter, M. A., Cullen, M. J., Baker, M. B., Hecht, R., Winters, D. et al (1995) Effects of the obese gene product on body weight regulation in *ob/ob* mice. Science 269, 540–543. PMID: 7624776
[27] Crane, J. D., Mottillo, E. P., Farncombe, T. H., Morrison, K. M., and Steinberg, G. R. (2014) A standardized infrared imaging technique that specifically detects UCP1-mediated thermogenesis *in vivo*. Mol. Metab. 3, 490–494. 24944909
[28] Landsberg, L., Saville, M. E., Young, J. B. (1984) The sympathoadrenal system and regulation of thermogenesis. Am. J. Physiol. 247, E181–E189. PMID: 6380306
[29] Fernández-Veledo, S., Vázquez-Carballo, A., Vila-Bedmar, R., Ceperuelo-Mallafré, V., and Vendrell, J. (2013) Role of energy- and nutrient-sensing kinases AMP-activated protein kinase (AMPK) and mammalian target of rapamycin (mTOR) in adipocyte differentiation. IUBMB Life 65, 572–583. PMID: 23671028
[30] Schneeberger, M., Gomis, R., and Claret, M. (2014) Hypothalamic and brainstem neuronal circuits controlling homeostatic energy balance. J. Endocrinol. 220, T25–T46. PMID: 24222039
[31] Hardie, D. G., Ross, F. A., and Hawley, S. A. (2012) AMPK: a nutrient and energy sensor that maintains energy homeostasis. Nat. Rev. Mol. Cell Biol. 13, 251–262. PMID: 22436748
[32] Thoreen, C. C., Chantranupong, L., Keys, H. R., Wang, T., Gray, N. S., et al (2012) A unifying model for mTORC1-mediated regulation of mRNA translation. Nature 485, 109–113. PMID: 22552098
[33] Ryan, K. K., and Seeley, R. J. (2013) Physiology. Food as a hormone. Science 339, 918–919. PMID: 23430646
[34] Schutz, Y., Byrne, N. M., Dulloo, A., and Hills, A. P. (2014). Energy gap in the aetiology of body weight gain and obesity: a challenging concept with a complex evaluation and pitfalls. Obes. Facts 7,15– 25. PMID:24457473
[35] Sjöström, L. (2013). Review of the key results from the Swedish Obese Subjects (SOS) trial—a prospective controlled intervention study of bariatric surgery. J. Intern. Med. 273,219–234. PMID: 23163728
[36] Dulloo, A. G. (2012) Explaining the failures of obesity therapy: willpower attenuation, target miscalculation or metabolic compensation?. Int. J. Obes. (Lond) 36, 1418–1420.
[37] Major, G. C, Doucet, E., Trayhurn, P., Astrup, A., and Tremblay, A. (2007). Clinical significance of adaptive thermogenesis. Int. J. Obes. 31, 204–212. PMID: 17260010